Journal of Medical Systems (2019) 43: 231
https://doi.org/10.1007/s10916-019-1373-7

IMAGE & SIGNAL PROCESSING

Diagnosis of Thyroid Nodules Based on Local Non-quantitative Multi-Directional Texture Descriptor with Rotation Invariant Characteristics for Ultrasound Image

Li Bi[1] · Zhang Shuang[1]

Received: 24 March 2019 / Accepted: 5 June 2019 / Published online: 14 June 2019

Abstract
The traditional texture feature lacks the directional analysis of graphical element, so it could not better distinguish the thyroid nodule texture image formed by the rotation of graphical element. A non-quantifiable local feature is adopted in this paper to design a robust texture descriptor so as to enhance the robustness of the texture classification in the rotation and scale changes, which can improve the diagnostic accuracy of thyroid nodules in ultrasound images. First of all, the concept of local feature with rotational symmetry is introduced. It is found that many rotation invariant local features are rotational symmetric to a certain degree. Therefore, we propose a novel local feature to describe the rotation invariant properties of the texture. In order to deal with the change of rotation and scale of ultrasound thyroid nodules in image, Pairwise rotation-invariant spatial context feature is adopted to analyze the texture feature, which can combine with the scale information without increasing the dimension of the local feature. The fadopted local features have strong robustness to rotation and gray intensity variation. The experimental results show that our proposed method outperforms the existing algorithms on thyroid ultrasound data sets, which greatly improve the Diagnosis accuracy of thyroid nodules.

Keywords Thyroid nodule · Texture descriptor · Non-quantitative · Multi-direction · SVM classifier · Rotation invariant · Local feature

Introduction

Thyroid diseases include diffuse thyroid disease and nodular thyroid diseases, both of them are harmful. Ultrasound examination is a commonly adopted method for diagnosis of thyroid diseases. Doctors provide a diagnostic result based on their knowledge and experience by observing the characteristics of ultrasound images. However, different doctors possess different experiences and backgrounds, the diagnostic results are not objective and consistency. Thus, an intelligent diagnostic technique, which can provide reliable diagnostic opinions of thyroid diseases based on ultrasound images, is needed to assist doctors in clinical diagnosis.

To implement a thyroid disease diagnosis system based on the research of ultrasound images of different thyroid diseases, scholars at home and abroad have proposed many effective algorithms. Because there is a significant difference between the ultrasonographic characteristics of benign and malignant thyroid nodules, so most of the existing algorithms perform texture feature analysis on tumor areas, and find out the difference between them to achieve accurate diagnosis of thyroid diseases. Literature [1] achieved the region of interest (ROI), preprocess and feature extraction of ultrasound thyroid images, where Multi-level Wavelet Multi-sub-bands Co-occurrence Matrix (MWMCM), fibrous variant texture and the longest highlighting run-length based on GLRL are proposed based on diffuse disease, while eccentricity and compactness of the nodule is extracted based on thyroid nodules. As for diffuse thyroid disease, a two-class classification method is proposed in [2], and the mRMR method is applied for feature selection, combining with SVM classifier, the

This article is part of the Topical Collection on *Image & Signal Processing*

✉ Li Bi
13941647321@163.com; lsunnyb@sina.com

[1] The First Affiliated Hospital of Jinzhou Medical University, Jinzhou 121001, Liaoning, China

classification accuracy are exceeding these algorithms with single-feature model.

Based on speckle noise, low contrast, inhomogeneity of the ultrasound image, geodesic active contour models (GAC), one of geometric active contour models, has been improved. The geometric active contour model based on the phase information (PCGAC) has been proposed. The model can segment the boundary contour of thyroid nodules. This GAC model based on gradient boundary is sensitive to noise and does not have the ability to detect weak edges. The Phase Congruency edge detection algorithm has better capability to detect noise images and weak edge. Some model construct the stop function based on the phase information, instead of the GAC model's edge stop function. The geodesic active contour segmentation model based on the Phase Congruency (PCGAC) has been received. The segmentation results explain the PCGAC model based on Phase Congruency is better than traditional GAC model, accuracy has been greatly enhanced.

Texture classification is a classic computer vision problem and has become a research hotspot in recent years. Many scholars have proposed a number of texture classification methods, where most of the research directions focus on the use of artificial intelligence methods to learn appropriate texture content representation methods. Potential texture features can be encoded regardless of changes in the scale, viewing angle, and rotation of the image texture [3]. Early thyroid diagnostic methods can take advantage of the simple statistical properties of texture images to obtain texture features, but cannot deal with the problems caadopted by environmental changes. Recently, most of the research work on texture classification is based on local features, and the local classification of texture images is adopted to make texture classification more robust to different ultrasound gray changes. A number of local features have been proposed to describe texture images, which can be roughly divided into three categories: 1) texture filtering based methods [4–6]; 2) binary pattern local feature based methods [7–9]; 3) texture gradient local features-based methods [10, 11]. The texture filtering based method describes the shape of the texture in terms of the distribution of the filter responses, such as the MR8 algorithm mentioned in Literature [12] and the basic BIFs feature algorithm mentioned in Literature [13].

However, it is not easy to select a filter bank that satisfies the texture characteristics, and these filters are closely related to the data type and cannot achieve universality. The binary mode is based on the binarized pixel grayscale difference that captures local structural features, including the Centrist feature [14], local binary mode (LBPs) [1] and its many improved algorithms [2, 15, 7]. Texture gradient local features, such as the SIFT algorithm [16] and the fractal-driven MSC algorithm [17], utilize the quantization gradient of the image block to describe the appearance of the texture region in thyroid lesions. It can be seen that since the local features based on the binary mode and the texture gradient contain a quantization step, the image information may be lost, resulting in erroneous classification results for thyroid nodule. The threshold value of the pixel difference may cause information loss in the binary mode local feature and in the texture gradient local features of SIFT and MFS, the coarse quantization of the gradient will result in the loss of information.

In order to reduce the classification error caadopted by the traditional texture, a novel local feature is proposed for diagnosis of ultrasound image [18, 11] which reduces the information loss caadopted by quantization and shows good performance. In addition, the pairwise rotation-invariant spatial context feature is constant when the gradation intensity changes. That is to say that it can achieve texture classification by capturing information at different scales, resolutions, and directions. Although pairwise rotation-invariant spatial context feature can have different scales of information at the micro and macro levels, pairwise rotation-invariant spatial context feature does not have rotational invariant, which limits its performance in some situations, such as medicine image. Due to the arbitrariness and diversity of ultrasound image content, rotation invariance is an important feature for texture descriptors. As can be seen from the descriptions in [2, 19], the introduction of rotational invariance into local features will improve the performance of their applications, especially for the description of thyroid lesions.

In this paper, we attempt to design a robust texture descriptor based on the non-quantized local feature. First, the concept of rotational symmetry of local features is introduced. It is found that many of the local features with rotation invariance are rotationally symmetric to some extent. Therefore, we propose new local features to describe the rotation invariant properties of the texture for thyroid lesions. In order to deal with the violent or sharp rotation, scale and other changes, the *spatial context* co-occurrence feature is adopted to perform multi-scale analysis on the texture feature quantity, which can combine with the scale information without increasing the dimension of the local feature. The resulting local features are robust to rotation and single intensity variations. The experimental results show that the evaluation indexes of our proposed method exceed the existing optimal algorithms on most ultrasound image, which greatly improves the texture classification effect.

Related works

Local binary pattern

The local binary pattern is a typical local texture descriptor, which encodes the image local texture information by comparing the gray relationship between the arbitrary pixel points of the image and its neighboring pixels [20–22]. If the gray value of the neighborhood pixel is greater than or equal to the

gray value of the central pixel, the position of the neighboring pixel is marked as 1, otherwise it is set to 0. In addition, different neighboring points are given different weights according to a specified coding strategy, where a binary sequence is converted to an unsigned decimal number and is adopted as the LBP feature of the pixel. The LBP feature is written as follows:

$$L_{R,P} = \sum_{i=0}^{P-1} s(g_i - g_c)2^i \tag{1}$$

$$s(x) = \begin{cases} 1 & x \geq 0 \\ 0 & x < 0 \end{cases} \tag{2}$$

where R represents the neighborhood radius; N represents the number of uniformly distributed pixels in the circular neighborhood with radius R, represents the gray value of the central pixel of the local neighborhood, and $g_i (i = 1, 2, \cdots, P-1)$ represents the gray value of the neighborhood pixel.

When the image rotation changes, the LBP value of pixel point will be changed [23]. In order to achieve the rotation invariance of the image, Ojal et al. [24] proposed a improved LBP operator with rotation invariant. The initial coding sequence of the circular neighborhood is continuously transformed to obtain a series of initially defined LBP value, and the minimum value is taken as the LBP value of the neighborhood, and the mathematical description can be expressed as

$$L_{R,P}^{ri} = \min\left\{ROR\left(L_{R,P}, i\right) | i = 0, 1, \cdots, P-1\right\} \tag{3}$$

where RO$R(x, i)$ denotes that the corresponding binary number is rotated with right-shift by i bits. By introducing the rotation invariant mode, the recognition performance of the LBP algorithm for the texture image with rotation change has been greatly improved, but with the increase of the number of neighborhood points, the feature dimension grows faster, while the too high feature dimension does not satisfy the timeliness of LBP algorithm and subsequent feature calculations and data storage requirements. Therefore, in order to further improve the LBP feature descriptor rotation-invariance and reduce the feature dimension, Ojal et al. proposed that the rotation invariant mode is divided into a rotation invariant uniform mode and a rotation invariant non-uniform mode on the basis of the number of 0/1 (or 1 / 0) transformations in the binary coding sequence, and the rotation invariant uniform mode is marked as the P + 1 class according to the number of binary numbers 1 in the sequence, all the rotation invariant non-uniform patterns are classified into one large class. The rotation invariant uniform mode of the LBP feature can be expressed as follows:

$$L_{R,P}^{riu2} = \begin{cases} \sum_{i=0}^{P-1} s(g_i - g_c) & U\left(L_{R,P}\right) \leq 2 \\ P+1 & else \end{cases} \tag{4}$$

$$U\left(L_{R,P}\right) = |s\left(g_{p-1} - g_c\right) - s(g_0 - g_c)| + \sum_{i=1}^{P-1} |s(g_i - g_c) - s(g_{i-1} - g_c)| \tag{5}$$

where U represents the number of 0/1 (or 1/0) transformations between two adjacent binary values in a binary sequence. In this paper, the number of neighborhood points P is 8, and the L^{riu2} feature dimension is 10.

Pairwise rotation-invariant spatial context feature

From the perspective of information theory, it is observed that two events with certain correlations can obtain more potentially useful information than they are observed to occur independently. Applying to texture classification, it is considered that the correlation feature between two features can describe a larger and more complex local texture structure than a single feature. Therefore, the literature [24] proposed an effective pairwise rotation-invariant context texture feature co-occurrence coding strategy. As for any pixel A in the image, two context co-occurrence points B and C are determined by calculating the unit gradient direction of the point A and the unit tangential direction, and the features of B and C points are coded according to the local texture structure information of point A. And then, the co-occurrence features of the two pairs (A, B) and (A, C) are adopted to describe the texture of the A point in the larger neighborhood. Its mathematical description can be expressed as

$$\begin{cases} CoLBP_{R,P}\left(A, \overline{B}\right) = \left[L_{R,P}^{u2}(A), L_{R,P}^{riu2}\left(\overline{B}, i(A)\right)\right]_{co} \\ i(A) = \text{argmax}\left(ROR\left(L_{R,P}(A), i\right)\right) \\ B = \alpha G(A) + bN(A) + A \\ \overline{B} = \phi(B) \end{cases} \tag{6}$$

where $L^{riu2}(A)$ is the local texture feature of point A, $i(A)$ is the starting code point number of the neighborhood corresponding to the maximum eigenvalue of point A, and $L_{R,P}^{riu2}\left(\overline{B}, i(A)\right)$ is the local texture feature corresponding to the coded starting point of the first $i(A)$ neighborhood point of the co-occurrence point $\overline{B}$. G(A) and $N(A)$ respectively represent the unit gradient direction of the pixel point A and the unit normal direction, and a and b represent scale templates for measuring the spatial distance between the co-occurrence point-pairs, which can be represented as respectively (3, 0) and (0, 3; ϕ is coordinate transformation function, which is to map the co-occurrence point B on the original image to the point $\overline{B}$ on the corresponding scale space image.

Materials and methods

Since the co-occurrence point-pair location selection in the original CoLBP algorithm is sensitive to image rotation changes, and the description of the context texture features is too single, the robustness to grayscale changes is weak. Aiming at these two problems, an improved non-quantized rotation invariant texture descriptor with low feature dimension and strong robustness to image rotation is designed [25]. The improved algorithm is recorded as enhanced non-quantized pairwise rotation-invariant LBP (ENPRL).

Improved spatial context co-occurrence feature

As the image rotates, the neighboring pixels around the pixel will change, that is to say that the gradient direction of the pixel will change after the rotation changes, which makes the original algorithm less robust to image rotation changes. However, the image rotation change can be regarded as only changing the position of the starting point of the neighborhood when the pixel is LBP encoded in the case of being unaffected by noise, while the neighborhood starting code point corresponding to the maximum and minimum values of the pixel LBP feature has not changed, as shown in Fig. 1. Therefore, the two co-directional direction vectors *m, n* are determined by the neighborhood coding starting point corresponding to the pixel point and its LBP feature extremum, and two co-occurrence points with the pixel point spatial context are determined in the two co-occurrence directions respectively. As shown in Fig. 1, since the LBP feature extremum of the pixel point A has rotation invariance corresponding to the neighborhood starting code point, the relative position between the co-occurrence point pairs (A, B) and (A, C) and their high-order angle features are not changed by the image rotation. Therefore, the spatial co-occurrence pixel points are calculated by using the two co-directional direction vectors *m, n* determined by the pixel starting point *A* and the neighborhood starting code point corresponding to the LBP feature extremum. The position can effectively enhance the robustness of the algorithm to image rotation changes. The mathematical description of the contextual co-occurrence point selection of the improved algorithm can be expressed as follows

$$\begin{cases} \mathrm{B} = \phi(A + \alpha f_{\max}(A) + bh_{\max}(A)) \\ \mathrm{C} = \phi(A + \alpha f_{\min}(A) + bh_{\min}(A)) \\ i_{\max}(A) = \operatorname{argmax}\left(\mathrm{ROP}\left(\mathrm{L}_{R,P}(\mathrm{A}), i\right)\right) \\ i_{\min}(A) = \operatorname{argmin}\left(\mathrm{ROP}\left(\mathrm{L}_{R,P}(\mathrm{A}), i\right)\right) \end{cases} \tag{7}$$

where $f(x)$ and $h(x)$ represent the direction vectors determined by the neighborhood starting code points corresponding to the maximum and minimum LBP values of pixel A, respectively; $i_{\max}(A)$and $i_{\min}(A)$ represent the sequence number of the neighborhood starting code point corresponding to the maximum and minimum values of the LB P feature of the pixel point A, respectively.

ELBP local texture features

In order to solve the problem that LBP algorithm is sensitive to texture nonlinear gray and rotation changes, an extended local binary binary (ELBP) is proposed in literature [26], which uses the joint distribution form of two complementary pixel grayscale and differential features to represent the local texture structure of the image. The pixel grayscale feature includes a local binary binary (NI-LBP) based on the gray of the neighborhood point, and a central pixel gray feature (CI-LBP); the pixel grayscale difference feature includes the radial difference local binary pattern (RD-LBP) and angular grayscale difference based local binary binary (AD-LBP). In this paper, the ELBP algorithm is introduced to extract the local neighborhood gray feature, the radial neighborhood gray difference feature and the central pixel gray feature, respectively. Compared with the original algorithm, the improved algorithm has a richer feature pattern. The ELBP mathematical description can be written as follows,

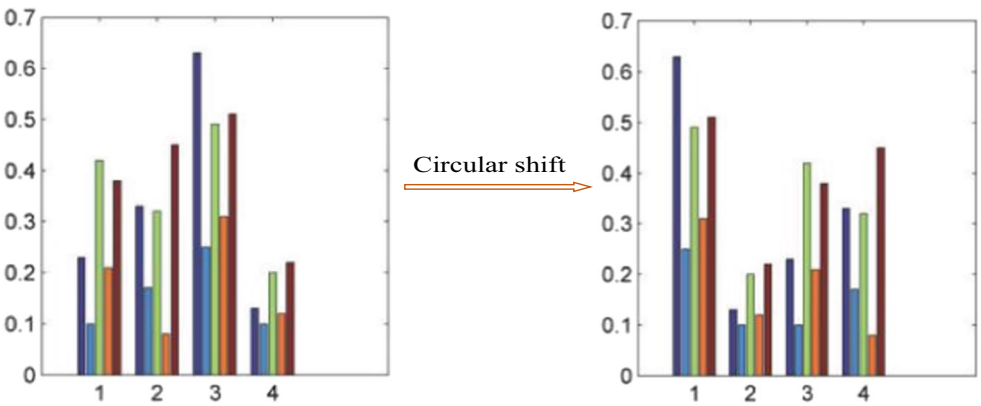

Fig. 1 Circular shift for LBP feature

$$\begin{cases} \mathrm{E} = N/R/C \\ N_{R,P} = \sum_{i=0}^{P-1} s(g_i - u_p)2^i, u_p = \frac{1}{P}\sum_{i=0}^{P-1} g_i \\ R_{R,P} = \sum_{i=0}^{P-1} s\left(\Delta_{\delta,i}^{Rad}\right)2^i, \Delta_{\delta,i}^{Rad} = x_{R,i} - x_{R-\delta,i} \\ C_{R,P} = s(g_c - u), u = mean(I(:)) \end{cases} \tag{8}$$

where u_p is the gray-scale mean of the neighboring pixel points, $\Delta_{\delta,i}^{Rad}$ is the gray-scale difference between the neighborhood points of the different neighborhood radius in the same radial direction; $\delta \in [1, P/2]$; u represents the gray-scale mean of the entire image.

Classification of thyroid nodules based on improved texture description operator

Thyroid disease diagnosis system

The basic principle of the thyroid disease diagnosis system is to extract the local texture features of the ultrasound image firstly, then learn the ELBP texture primitives from these local features, then use these texture primitives to encode the texture image. Finally, the classifier is adopted to perform texture classification to achieve the thyroid disease diagnosis. The system block diagram is shown in Figs. 1 and 2.

Non-quantized rotation invariant texture feature fusion

Texture feature extraction methods can be divided into four categories: statistical methods, structural (geometric) methods, model methods, and methods based on mathematical transformations (signal processing). In this paper, the gray level co-occurrence matrix based on the statistical method is adopted to obtain the texture information. The gray level co-occurrence matrix describes the spatial distribution and structural features of the gray levels of each pixel in the image, and the texture features are adopted to improve the classification accuracy of the thyroid region. Non-quantized rotation invariant texture feature fusion is defined as the probability of a point from a gray i from a fixed position relationship$d = (D_x, D_y)$ to a gray$j$, and can be represented as $p_{ij}(d)$ $(i, j = 1, 2, \cdots, L-1)$, whichLis the gray level of the image; i, j represents the gray level of the pixel, respectively; d represents the spatial positional relationship between the two pixels, different d determines the distance and direction between the two pixels; θ is the direction of generation of the gray level co-occurrence matrix, usually taken 4 directions 0°, 45°, 90° and 135°.

Due to the large amount of the ultrasound image data and the computational complexity of the texture feature extraction algorithm based on the gray level co-occurrence matrix, four simple texture features such as ASM, Entropy, contrast and correlation represent the uniformity, complexity, sharpness and linearity of the texture features, which are better and less time-consuming for texture analysis. These four features are fadopted with our proposed pairwise non-quantized rotation-invariant spatial context feature to enhance the characterization of thyroid texture. The specific meanings and parameters of the four common features are calculated as follows:

1) Angular Second moment (ASM): Reflecting the uniformity of image gray distribution, the energy moments of coarse texture are larger than those of fine texture, while the energy moments of fine texture are smaller.

$$f_{ASM} = \sum_{i=0}^{L-1}\sum_{j=0}^{L-1} p_d^2(i,j) \tag{9}$$

2) Entropy (ENT): It measures the amount of information of an image. If the image does not have any texture, the entropy is close to zero; if the image is full of fine texture, the image entropy value is the largest; if the image has less texture, the image has a smaller value.

$$f_{ENT} = -\sum_{i=0}^{L-1}\sum_{j=0}^{L-1} p_d(i,j)\lg p_d(i,j) \tag{10}$$

3) Contrast (CON): Contrast reflects the sharpness of the image texture, the deeper the groove of the texture, the greater the contrast, the better the visual clarity of the image.

$$f_{CON} = \sum_{n=0}^{L-1} n^2 \left[\sum_{i=0}^{L-1}\sum_{j=0}^{L-1} p_d(i,j)\right] \tag{11}$$

4) Correlation (COR): The degree of similarity of the gray level co-occurrence matrix elements in the row or column direction is measured, and the correlation magnitude

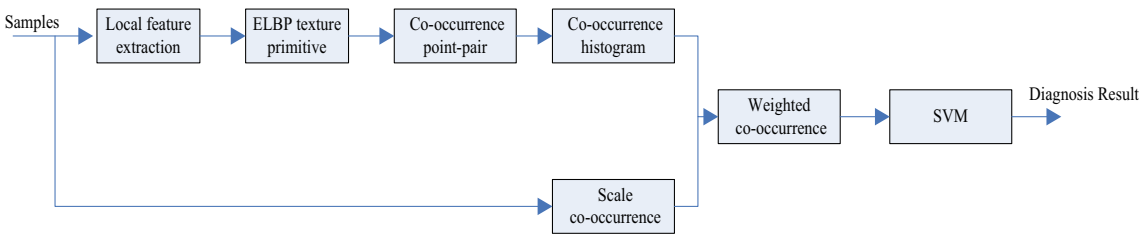

Fig. 2 The basic principle of the thyroid disease diagnosis system

reflects the degree of correlation of the local gray levels in the image.

$$f_{COR} = \sum_{i=0}^{L-1}\sum_{j=0}^{L-1}\frac{ijp_d(i,j)-u_1u_2}{\sigma_1^2\sigma_2^2} \tag{12}$$

where,

$$u_1 = \sum_{i=0}^{L-1} i \sum_{i=0}^{L-1}\sum_{j=0}^{L-1} p_d(i,j) \tag{13}$$

$$u_2 = \sum_{j=0}^{L-1} j \sum_{i=0}^{L-1}\sum_{j=0}^{L-1} p_d(i,j) \tag{14}$$

$$\sigma_1 = \sum_{i=0}^{L-1} (i-u_1)^2 \sum_{j=0}^{L-1} p_d(i,j) \tag{15}$$

$$\sigma_2 = \sum_{i=0}^{L-1} (i-u_2)^2 \sum_{j=0}^{L-1} p_d(i,j) \tag{16}$$

SVM classifier

SVM is a classification model derived from statistical theory from the optimal hyperplane in the case of linear separability [27]. This paper uses SVM to classify the extracted features to achieve the diagnosis of thyroid nodules. The basic principle is classify the training sample set to two types, which can be denoted as (x_1, y_1), (x_2, y_2), $\cdots$, (x_k, y_k), $y \in \{+1, -1\}$.

These samples can be separated by a hyperplane, which can be written as

$$W\phi(x) + b = 0 \tag{17}$$

where W is weight vector for classification plane; b is offset, $b \in R$;ϕ is the mapping of the input feature space to the high-dimensional Hilbert space (H), where the optimal classification hyperplane is constructed in this space.

$$\phi : \mathrm{R}^n \rightarrow H \tag{18}$$

The process of finding the optimal classification hyperplane can be transformed into solving an optimization problem, which can be expressed as eqs. (8) and (9) called objective functions and constraints, respectively.

$$\min_{W,b,\varsigma} \frac{1}{2}\|W\|^2 + C\sum_{i=1}^{K}\xi_i \tag{19}$$

$$y_i(W\phi(x_i) + b) + \varsigma_i \geq 1 \tag{20}$$

where ς_i is slack variable, $\varsigma_i \geq 0 (i = 1, 2, \cdots, k)$; C is penalty coefficient.

The introduction of slack variables and penalty coefficients is to solve the linear indivisible problem of the data set. To understand the above optimization problem, the Lagrange function is adopted to transform the original optimization problem into a dual optimization problem. The objective function and constraints can be expressed as

$$\max L(a) = \sum_{i=1}^{k}\alpha_i - \frac{1}{2}\sum_{i=1}^{k}\sum_{j=1}^{k} a_i a_j y_j y_i K(x_i, x_j) \tag{21}$$

$$\sum_{i=1}^{k} y_i\alpha_i = 0, \alpha_i \geq 0, i = 1, 2, \cdots, k \tag{22}$$

$\mathrm{K}(x_i, x_j)$ is a kernel function. The kernel function is adopted to map the input feature space to a high-dimensional space. The kernel function adopted by the SVM algorithm must satisfy the Mercer theorem, which is the matrix must be semi-positive. Commonly adopted kernel functions include polynomial functions and radial basis functions (RBF), they are respectively written as follow

$$\mathrm{K}(x_i x_j) = (x_i x_j + 1)^p \tag{23}$$

$$\mathrm{K}(x_i x_j) = e^{-\gamma(x_i - x_j)^2} \tag{24}$$

In our thyroid disease diagnosis system, SMO is adopted to solve the above dual problem, the optimal solution is $a^0 = (a_1^0, a_2^0, \cdots, a_k^0)$. It is concluded that the discriminant function of SVM classification is written as follows:

$$f(x) = \mathrm{sgn}(\sum y_i a_i^0 K(x_i x) - b^0) \tag{25}$$

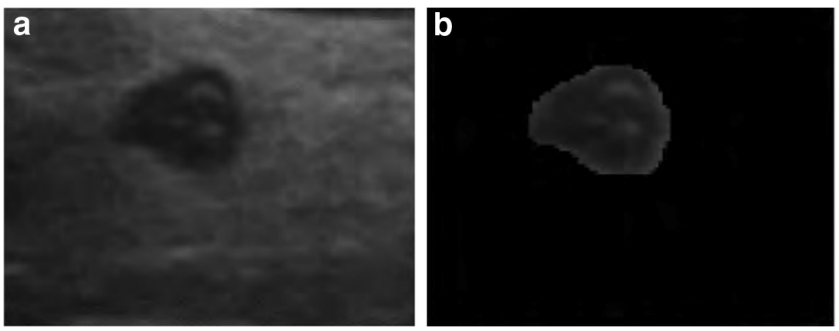

Fig. 3 Thyroid ultrasound image of the lesion area; (a) original image; (b) Lesion area

Table 1 P value and *AUC* values of the mean and variance of the feature parameters

	P value	*AUC*		P value	*AUC*
ENGMEAN	<0.000 1	0.928	CONVAR	<0.000 1	0.901
ENGVAR	<0.000 1	0.801	CORMEAN	<0.000 1	0.894
ENTMEAN	<0.000 1	0.952	CORVAR	<0.008 0	0.766
ENTVAR	<0.000 1	0.880	HOMMEAN	<0.000 1	0.928
CONMEAN	<0.000 1	0.919	HOMVAR	<0.000 1	0.910

Experiment results

The ultrasound images of the 500 thyroid nodules selected in the experiment are from a 3A Grade hospitals, where 100 images are benign nodules, and the other 100 images are malignant. All images have corresponding B-ultrasound reports and pathological examination reports. The nodule area and boundary are marked by the clinician. Since the gray level is large, it is necessary to perform gray quantization on the image. The original image contains the region of interest and most of the non-interest region, which needs to extract ROI region. The specific operation is to manually segment the normal and lesion areas from the ultrasound image of the thyroid patient by referring to the lesion area outlined by the doctor. Figure 3 shows the thyroid ultrasound image of the lesion area that the doctor has outlined. Figure 3(b) shows the white outline delineation area in 3(a). The adopted ultrasound diagnostic instrument is the Philips iu22 color ultrasound diagnostic probe, where the frequency is 7 MHz~12 MHz. The experimental platform is Windows 10 Professional PC. The processor is Intel(R) core(TM) i5–4600@3.2GHz, the memory is 4GB, and the simulation software is MATLAB 2013a (64 bit).

Evaluation indexes

Logistic regression model is mainly adopted in medicine to predict the probability of a disease occurring. Binary logistic regression analysis has been widely adopted in the field of medical research, including the prediction and discrimination of diseases. In order to verify the effectiveness of the proposed algorithm, 500 thyroid ultrasound images are adopted to extract the texture features. Logistic regression is based on the gold standard diagnosis results [28]. The extracted texture feature parameters are adopted as covariates to establish a logistic regression model so as to obtain sensitivity, specificity, accuracy, and the missed diagnosis rate, misdiagnosis rate and area under the ROC curve(AUC) [2, 20, 29]. Sensitive (Sen) refers to the percentage of the actual diagnosis that is correctly diagnosed, and its formula is written as follows;

$$\mathrm{SENS} = \frac{TP}{TP + FN} \tag{26}$$

The rate of missed diagnosis is not detected. The rate of missed diagnosis is *1-Sen*. The specificity (Spe) reflects the ability of the diagnostic experiment to exclude *normal-cases*, whose equation is written as:

$$SPEC = \frac{\mathrm{TN}}{TN + FP} \tag{27}$$

The rate of misdiagnosis did not exclude the proportion of normal-cases, the rate of misdiagnosis is *1-Spe*; the accuracy (Accuracy, Acc) reflects the ability to correctly diagnose normal and pathological changes, and the formula is as follows

$$\mathrm{ACC} = \frac{TP + TN}{TP + FP + FN + TN} \tag{28}$$

In these formulas, ACC, SENS and SPEC indicate the accuracy, sensitivity and specificity, respectively; TP, TN, FP and FN are indicated as the number of true positive, true negative, false positive and false negative, respectively.

Another evaluation index is the area under the ROC curve (AUC), which is calculated as the following equation

$$\mathrm{AUC} = \frac{1 + TP_{rate} - FP_{rate}}{2} \tag{29}$$

where $TP_{rate} = Sen$ and $FP_{rate} = 1 - Spe$. When the value of AUC is 0.5~0.7, the diagnostic value is low; 0.7~0.9 means that the diagnostic value is medium; when it is above 0.9, the diagnostic value is higher. The above six evaluation indicators are adopted to determine the performance of the thyroid lesion. According to the above rules, binary Logistic regression model analysis and ROC curve analysis are adopted to analyze the significance of each parameter of the algorithm, namely, p value, which is clinically significant when $p < 0.05$. To evaluate the accuracy for classification of thyroid images, the greater the AUC value, the greater the clinical

Table 2 Recognition rate for different algorithms

Groups	LBP	LTP	LBPV	CLBP	CLBC	CoLBP	ELBP	Proposed
A	78.16	96.81	87.38	96.66	95.72	97.59	97.21	97.35
B	67.06	83.98	71.65	91.82	91.35	88.54	91.04	93.24
C	78.24	92.35	82.61	96.74	96.55	92.68	96.34	97.30
D	76.95	94.46	94.12	97.05	97.35	95.98	97.10	97.21

Table 3 The recognition rates of different algorithm on C and D groups

Methods	LBP	LTP	LBPV	CLBP	CLBC	CoLBP	ELBP	Proposed
C	87.39	97.62	99.18	99.36	99.65	99.71	99.42	99.79
D	88.62	95.84	98.42	99.36	99.48	99.67	99.28	99.81
Means	88.69	95.70	98.48	99.16	99.42	99.57	99.18	99.80

significance. The higher the specificity and sensitivity, the lower the probability of diagnosis and missed diagnosis.

Experimental analysis

Experiments select the original LBP [19], ELBP [3], CMLBP [16] as comparative algorithms for performance analysis. The binary logistic regression model is adopted to analyze the accuracy, sensitivity, specificity, missed diagnosis rate, misdiagnosis rate and area under the ROC curve. Since there are many experimental data, we use grouping strategy to make independent experiments. All data are divided into 5 groups: A, B, C and D, each of which had 60 normal images, 20 benign images, and 20 malignant ultrasound images. The improved texture feature extraction of the matrix algorithm for lesions and normal regions is performed respectively, and the mean and variance of feature vectors: ENG, ENT, HOM, CON and COR are obtained. Table 1 shows the *P* value and *AUC* values of the mean and variance of the feature parameters ENG, ENT, HOM, CON and COR of the algorithm.

It is obvious that the P value of the parameters extracted by our proposed method is less than 0.0001 and has clinical diagnostic significance. According to the ROC curve and the AUC values in Table 1, the AUC values for energy, entropy, contrast, and ASM are higher, and the associated AUC values are relatively low. To compare the mean values of the feature parameters (energy, entropy, contrast, correlation, and ASM) of lesions and normal thyroid ROIs, we performed statistical analysis to compare. Obviously, the energy, entropy, contrast and ASM are more relevant to the differential diagnosis of the thyroid image in this experiment. The mean range of energy mean range: normal thyroid in 0.06~0.14, lesion in 0.01~0.05; similarly, entropy mean: normal in 2.2~3.3, lesion in 3.3~5.4; contrast mean: normal in 0.1~0.6, lesion in 2~ 8 fluctuations up and down; correlation mean: lesions in 0~0.2; mean ASM normal in 0.7~0.95, lesions fluctuating from 0.4~0.6. Comprehensive analysis, energy, entropy, contrast and moment of inertia are more relevant for the significance and diagnostic value of thyroid image prediction classification. It can be seen from the classification data in Table 2 that the recognition rate of our proposed algorithm is 0.32% higher than that of the original CoLBP algorithm and 0.49% higher than that of the ELBP algorithm, which is indicating that the local ELBP feature of the co-occurrence pixel is effective. The identification performance of our algorithm is enhanced. For the A-group data classification, the proposed algorithm classification rate is 1.39%, 1.96%, 5.62%, 2.96% higher than the CLBP, CLBC, CoLBP, and ELBP algorithms, respectively. The robustness to grayscale changes is strong. For the B-group texture images with scale and viewing angle changes, the recognition rate of CoELBP algorithm is 0.6%, 0.94%, 4.75%, 0.93% higher than CLBP, CLBC, CoLBP [7] and ELBP algorithms, respectively. It is indicated that the CoELBP algorithm is robust to texture rotation changes, especially on the C-group where all of samples have rotation and scale changes.

The algorithm recognition rate is 0.89%, 0.44%, 2.1%, and 0.83% higher than CLBP, CLBC, CoLBP, and ELBP, indicating that the proposed algorithm uses the neighborhood starting code point and neighborhood corresponding to the pixel local feature extremum. The context co-occurrence point pairs are determined, and the neighborhood gray information and radial gradation difference information of the context co-occurrence point are extracted by ELBP algorithm, which can effectively enhance the robustness of the algorithm to the rotation change.

It can be seen from the classification data in Table 3 that the average recognition rate of the original CoLBP algorithm is higher than that of the LBP and its improved algorithm for the C-group and D-group texture image classifications with obvious rotation changes, indicating that the higher order is obtained by coding the co-occurrence point pairs. The angle information improves the robustness of the algorithm to rotational variations. However, the original CoLBP algorithm calculates the gradient vector of the position of the co-occurrence

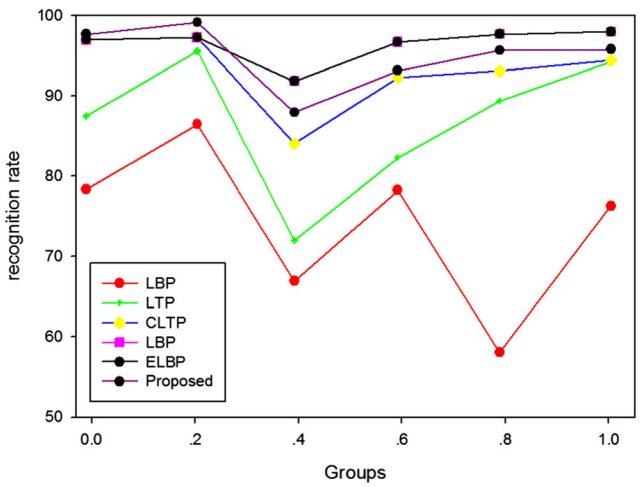

Fig. 4 The comparison of classification recognition rate on different algorithm

Table 4 The computational complexity of different algorithm on D database

Methods	LBP	LTP	LBPV	CLBP	CLBC	CoLBP	ELBP	Proposed
Feature dimension	10	100	10	200	163	200	180	600
Times	262.75	60.56	479.72	42.69	44.78	43.38	63.52	47.92

point of the scene and changes with the rotation of the image, so that the extracted high-order angle information will be distorted due to the rotation of the image. The algorithm uses the extreme value of the LBP feature. The strategy determines the direction of the co-occurrence vector, and ensures the stability of the high-order angle information between the co-occurrence point pairs obtained by the algorithm, so that the improved texture algorithm has a higher average recognition rate than the original algorithm. It is effective to demonstrate that the proposed algorithm is more robust to image rotation changes than the original CoLBP algorithm.

Figure 4 shows the comparison of the texture classification recognition rates of various LBP improved algorithms on different databases. It can be seen that the algorithm recognition rate is higher than that of the remaining LBP algorithms on the ultrasound database with rotation changes in the sample, which indicates that the algorithm is robust to image rotation changes. At the same time, it has C and complex texture changes. In group D, the recognition rate of this algorithm is higher than that of CoLBP algorithm and ELBP algorithm, which indicates that the co-occurrence point pairs on different scales and the complementary co-occurrence of fusion are selected by calculating the neighborhood starting code points corresponding to the pixel local feature extremum. The point-to-point ELBP texture feature effectively improves the robustness of the original algorithm to rotational changes.

Table 4 gives a comparison of the computational complexity of different algorithms on the D group, where the classification time represents the total time mean of 100 feature classification experiments, including the time of the classifier (SVM) model training and feature prediction. It can be seen from the data in the table that although the original CoLBP algorithm and the proposed algorithm have higher feature dimensions than the rest of the LBP algorithm, they have rich feature patterns due to their use of context s points to describe the texture structure. The feature classification time is less; in this paper, the ELBP operator is adopted to extract the neighborhood gray information and radial gray difference information of the context co-occurrence point, and the rotation invariant uniform mode is adopted to encode a single NI-LBP and RD-LBP feature reduces the feature dimension of the original CoLBP algorithm from 1180 to 600, and the feature classification time is reduced by 15.67 ms compared with the CoLBP algorithm, which greatly improves the computational efficiency and classification accuracy of the algorithm.

Conclusion

The traditional texture feature lacks the directional analysis of graphical element, so it could not better distinguish the thyroid nodule texture image formed by the rotation of graphical element. A non-quantifiable local feature is adopted in this paper to design a robust texture descriptor so as to enhance the robustness of the texture classification in the rotation and scale changes, which can improve the diagnostic accuracy of thyroid nodules in ultrasound images. First of all, the concept of local feature with rotational symmetry is introduced. It is found that many rotation invariant local features are rotational symmetric to a certain degree. Therefore, we propose a novel local feature to describe the rotation invariant properties of the texture. In order to deal with the change of rotation and scale of ultrasound thyroid nodules in image, pairwise rotation-invariant spatial context feature is adopted to analyze the texture feature, which can combine with the scale information without increasing the dimension of the local feature. The fadopted local features have strong robustness to rotation and gray intensity variation. The experimental results show that our proposed method outperforms the existing algorithms on thyroid ultrasound data sets, which greatly improve the Diagnosis accuracy of thyroid nodules.

Compliance with Ethical Standards

Conflict of Interest We declare that we have no conflict of interest. The paper does not contain any studies with human participants or animals performed by any of the authors. Informed consent was obtained from all individual participants included in the study.

References

1. Ojala, T., Pietikäinen, M., and Mäenpää, T., Multiresolution gray-scale and rotation invariant texture classification with local binary patterns. *IEEE Trans. Pattern Anal. Mach. Intell.* 24(7):971–987, 2002.
2. Ardakani, A. A., Gharbali, A., and Mohammadi, A., Classification of benign and malignant thyroid nodules using wavelet texture analysis of sonograms[J]. *J. Ultrasound Med.* 34(11):1983–1989, 2015.
3. Cross, G. R., and Jain, A. K., Markov random field texture models. *IEEE Trans. Pattern Anal. Mach. Intell.* PAMI-5(1):25–39, 1983.
4. Jang, M., Kim, S. M., Lyou, C. Y. et al., Differentiating benign from malignant thyroid nodules[J]. *J. Ultrasound Med.* 31(2):197–204, 2012.

5. Haralick, R. M., Shanmugam, K., and Dinstein, I. H., Textural features for image classification. *IEEE Trans. Syst. Man Cybern.* SMC-3(6):610–621, 1973.
6. Calonder, M., Lepetit, V., Strecha, C., and Fua, P., Brief: Binary robust independent elementary features. Proc. Eur. Conf. Computer Vision (ECCV). 778–792, 2010.
7. Mehta, R., Egiazarian, K., Texture classification using dense micro-block difference (DMD). *Proc. Asian Conf. Comput. Vis.* 1643–1658, 2014.
8. Perronnin, F., Sánchez, J., and Mensink, T., Improving the fisher kernel for large-scale image classification. *Proc. Eur. Conf. Comput. Vis.* 143–156, 2010.
9. Qian, P., Zhao, K., Jiang, Y., Kuan-Hao, S., Deng, Z., Wang, S., and Jr, R. F. M., Knowledge-leveraged transfer fuzzy c-means for texture image segmentation with self-adaptive cluster prototype matching. *Knowledge-Based Syst.* 130:33–50, 2017.
10. Weyl, H., Symmetry. Vol. 11. Princeton, NJ, USA: Princeton Univ. Press, 1952.
11. Xu, Y., Yang, X., Ling, H., and Ji, H., A new texture descriptor using Mul-tifractal analysis in multi-orientation wavelet pyramid. *Proc. IEEE Conf. Comput. Vis. Pattern Recog.* 161–168, 2010.
12. Varma, M., and Zisserman, A., A statistical approach to texture classification from single images. *Int. J. Comput. Vis.* 62(1–2):61–81, 2005.
13. Crosier, M., and Griffin, L. D., Using basic image features for texture classification. *Int. J. Comput. Vis.* 88(3):447–460, 2010.
14. Wu, J., and Rehg, J. M., Centrist: A visual descriptor for scene categorization. *IEEE Trans. Pattern Anal. Mach. Intell.* 33(8): 1489–1501, 2011.
15. Nixon, I. J., Ganly, I., Hann, L. E. et al., Nomogram for predicting malignancy in thyroid nodules using clinical, biochemical, ultrasonographic, and cytologic features[J]. *Surgery* 148(6):1120–1128, 2010.
16. Ivanac, G., Brkljacic, B., Ivanac, K. et al., Vascularisation of benign and malignant thyroid nodules: CD US evaluation.[J]. *Ultraschall in Der Medizin* 28(05):502–506, 2007.
17. Bo, Z., Yu-Xin, J., and Qing, D., et al., Prospective observation of contrast-enhanced patterns of thyroid nodules with SonoVue[J]. Chinese Journal of Medical Imaging Technology, 2010.
18. Nixon, I. J., Ian, G., Hann, L. E. et al., Nomogram for selecting thyroid nodules for ultrasound-guided fine-needle aspiration biopsy based on a quantification of risk of malignancy[J]. *Head Neck* 35(7):1022–1025, 2013.
19. Heng, Z, and Zheng, S., Research Progress of texture analysis in thyroid nodule imaging[J]. Chinese computed Medical Imaging, 2018.
20. Xia, Kai-Jian; Yin, Hong-Sheng; Rong, Gong-Sheng; Wang, Jiang-Qiang; Jin, Yong. X-ray image enhancement base on the improved adaptive low-pass filtering. *J. Med. Imaging Health Inform.*, Volume 8, Number 7, September 2018, pp. 1342–1348(7), doi: https://doi.org/10.1166/jmihi.2018.2472
21. Cimpoi, M., Maji, S., Kokkinos, I., Mohamed, S., and Vedaldi, A., Describing textures in the wild. *Proc. IEEE Conf. Comput. Vis. Pattern Recog.* 3606–3613, 2014.
22. Varma, M., and Zisserman, A., A statistical approach to material classifi-cation using image patch exemplars. *IEEE Trans. Pattern Anal. Mach. Intell.* 31(11):2032–2047, 2009.
23. Qian, P., Xi, C., Min, X., Jiang, Y., Kuan-Hao, S., Wang, S., and Jr, R. F. M., SSC-EKE: Semi-supervised classification with extensive knowledge exploitation. *Inform. Sci.* 422:51–76, 2018.
24. Ojal, L. X., Li, Z. et al., Real-time ultrasound Elastography in the differential diagnosis of benign and malignant thyroid nodules[J]. *J. Ultrasound Med.* 28(7):861–867, 2009.
25. Xia, K.-j., Yin, H.-s., and Zhang, Y.-d., Deep semantic segmentation of kidney and space-occupying lesion area based on SCNN and ResNet models combined with SIFT-flow algorithm. *J. Med. Syst.* 43:2, 2019. https://doi.org/10.1007/s10916-018-1116-1.
26. Moon, W. J., Jung, S. L., Lee, J. H. et al., Benign and malignant thyroid nodules: US differentiation–multicenter retrospective study.[J]. *Radiology* 247(3):762, 2008.
27. Urbach, E. R., Roerdink, J. B., and Wilkinson, M. H., Connected shape-size pattern spectra for rotation and scale-invariant classification of gray-scale images. *IEEE Trans. Pattern Anal. Mach. Intell.* 29(2):272–285, 2007.
28. Chen, J. et al., WLD: A robust local image descriptor. *IEEE Trans. Pattern Anal. Mach. Intell.* 32(9):1705–1720, 2010.
29. Sharma, G., ul Hussain, S., and Jurie, F., Local higher-order statistics (LHS) for texture categorization and facial analysis. *Proc. Eur. Conf. Comput. Vis.* 1–12, 2012.